

# CO Observations of Edge-on Galaxies. V. NGC 5907: Central Deficiency of Gas in an Sc Galaxy-Merger in the Bulge?

Yoshiaki SOFUE

*Institute of Astronomy, The University of Tokyo, Mitaka, Tokyo 181**E-mail sofue@sof.mtk.ia.s.u-tokyo.ac.jp*

(Received 1993 October 12; accepted 1993 November 9)

## Abstract

The edge-on Sc galaxy NGC 5907 has been observed in the  $^{12}\text{CO}(J=1-0)$ -line emission using the Nobeyama 45-m telescope. The radial density distribution at between 2 and 13 kpc is well represented by a superposition of an exponential-law disk of scale radius 3.5 kpc and a ring of 7 kpc radius. However, no concentration of gas has been observed in the central 2 kpc. The radial distribution and position-velocity diagram are compared in detail with those obtained for HI. We found that the molecular gas dominates in the central 5 kpc region, while HI dominates in the outer region, clearly separated by a “molecular front” at 5 kpc radius. This molecular front could be the place where the phase change from HI to  $\text{H}_2$ , or vice versa, is taking place on a galactic scale. The central deficiency of the molecular gas is exceptional for a late-type galaxy, which was found for the first time among Sc galaxies, and the second case after the Sb galaxy M31. We argue for the possibility of destruction of the nuclear gas disk by a merger with another galaxy, and discuss its relation to the outer warping disk.

**Key words:** CO emission — Galaxies — HI gas — Interstellar matter — Molecular hydrogen

## 1. Introduction

NGC 5907 is a nearby Sc galaxy with an almost edge-on orientation at an inclination angle of  $88^\circ$  (Sasaki 1987; Barnaby, Thronson 1992). Radio continuum maps have revealed a thin disk of nonthermal as well as thermal emissions (e.g., Hummel et al. 1984). Observations of the HI line emission have shown a large disk of interstellar gas, which is warping in the outermost regions (Sancisi 1976; Rots 1980; Bosma 1981).  $\text{CO}(J=1-0, 2-1)$  line emissions have been detected (Braine et al. 1993), while no mapping observations with a sufficient resolution have been obtained.

This paper is the fifth in a series describing the results of a high-resolution survey of edge-on galaxies in the  $^{12}\text{CO}(J=1-0)$  line emission using the Nobeyama 45-m telescope; we describe the results for NGC 5907. In our Papers I to IV we presented the results for other edge-on galaxies (Sofue et al. 1987, 1989; Sofue, Nakai 1993, 1994).

## 2. Observations

Observations of the  $^{12}\text{CO}(J=1-0)$  line emission of NGC 5907 were performed in 1992 December using the 45-m telescope of the Nobeyama Radio Observatory. The parameters for the galaxy are given in table 1. The observational parameters were described in Papers III and

IV in detail, and are summarized in table 2.

We used a coordinate system  $(X, Y)$  based on the distances along the major and minor axes from the center position, respectively ( $X$  is positive toward the south-east, and  $Y$  is positive toward the north-east). Observations were made at every  $15''$  grid interval along the major axis from  $X = -4'$  to  $+4'$ , which yielded an effective angular resolution of  $\theta = (\text{HPBW}^2 + \Delta X^2)^{1/2} = 21''$ , except for the edge-most region at  $|X| > 3'$ , where the interval was  $30''$ . Additional  $Y$  scans were made at several  $X$  positions in order to confirm that the CO intensity had a sharp maximum near to the adopted major axis.

## 3. Results and Discussion

### 3.1. Spectra and Position-Velocity Diagram

The obtained spectra are shown in figure 1. The CO emission has been detected at almost all positions, except for the edge-most few points. The spectra obtained by scans in the  $Y$  direction at some  $X$  positions indicate that the emission has a maximum at the adopted galactic plane. However, the present data are too crude to argue for a thick disk or a halo due to the insufficient coverage of the  $Y$  distance ( $\pm 15''$ ). Although a warping of the outermost part at  $|X| > 4'$  has been reported (Sasaki 1987), our data do not cover this area.

Using the data, we obtained a position-velocity (PV) diagram, which is shown in figure 2. The data were

Table 1. Parameters for NGC 5907.

Galaxy type .....	Sc; edge-on	
Center position ( $X = 0''$ , $Y = 0''$ )		(NED*)
R.A. <sub>1950</sub> .....	15 <sup>h</sup> 14 <sup>m</sup> 34 <sup>s</sup> .80	
Decl. <sub>1950</sub> .....	56°30'33".0	
Major axis P.A. ....	156°	(Sasaki 1987)
Inclination angle ..	88°	(Sasaki 1987)
Systemic $V_{LSR}$ .....	685 ( $\pm 5$ ) km s <sup>-1</sup>	(Present CO result)
$V_{rot}$ .....	225 ( $\pm 5$ ) km s <sup>-1</sup>	(Present CO result)
Distance .....	11.6 Mpc	(Schöniger, Sofue 1994)
CO luminosity <sup>†</sup> .....	$2.43(\pm 0.09) \times 10^8$ K km s <sup>-1</sup> pc <sup>2</sup>	
H <sub>2</sub> mass .....	$1.37(\pm 0.05) \times 10^9 M_{\odot}$	Conversion factor from Sanders et al. (1984)

\* NASA/IPAC Extragalactic Database (NED) (1992) (operated by JPL, Cal. I. Tech. under contract by NASA).

† Values in a "thin" disk of 27 kpc  $\times$  844 pc

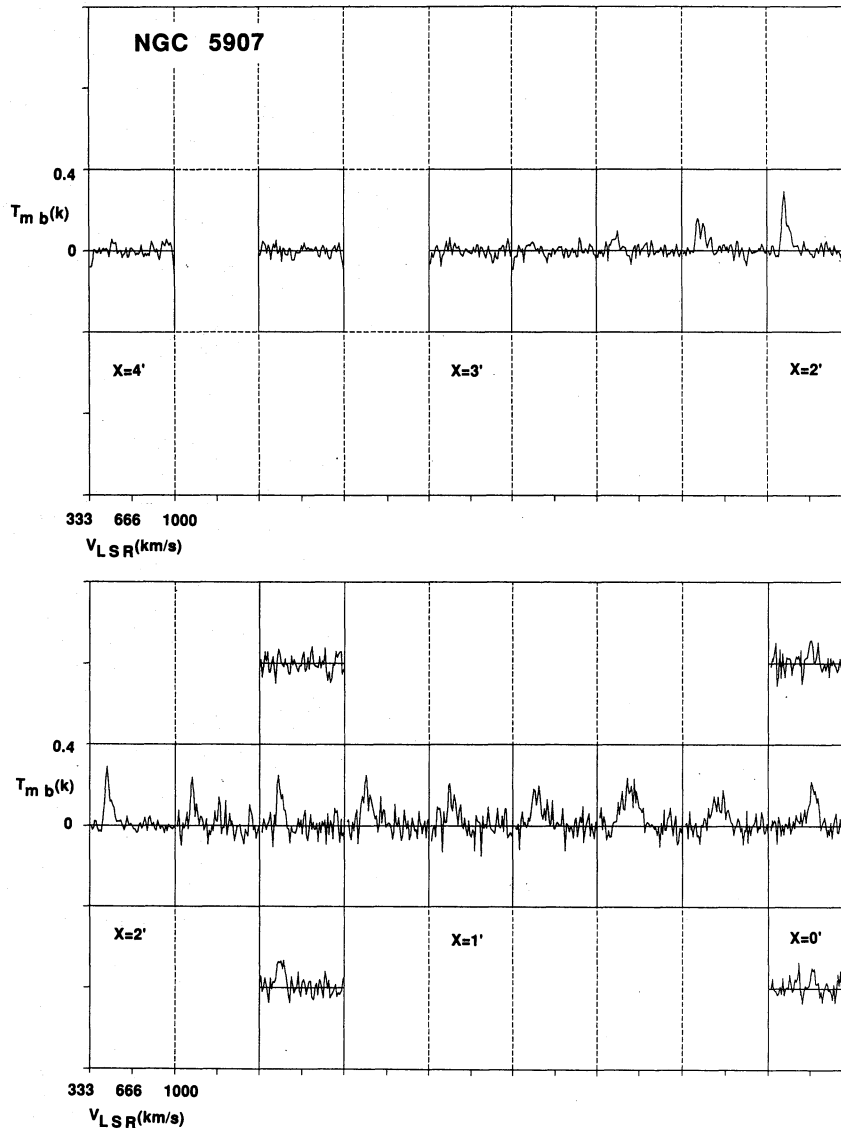


Fig. 1.  $^{12}\text{CO}(J=1-0)$  line spectra of NGC 5907 as observed by the 45-m telescope at Nobeyama.

Table 2. Observational parameters.

Telescope .....	Nobeyama 45-m telescope
Angular resolution (HPBW) .....	15'' (844 pc)
Pointing accuracy .....	$\pm 3''$ (calibrated by SiO masers)
Aperture efficiency .....	0.35
Main-beam efficiency .....	0.50
Integration time per point .....	5 to 10 min.
Velocity resolution .....	10 km s <sup>-1</sup> (32-ch binding from 2048-ch AOS)
Receiver system temperature .....	400–500 K (SIS receiver; SSB)
Rms of each spectra (10 km s <sup>-1</sup> resolution) .....	20 mK in $T_{mb}$
Rms on PV diagram (20'' $\times$ 20 km s <sup>-1</sup> ) .....	12 mK

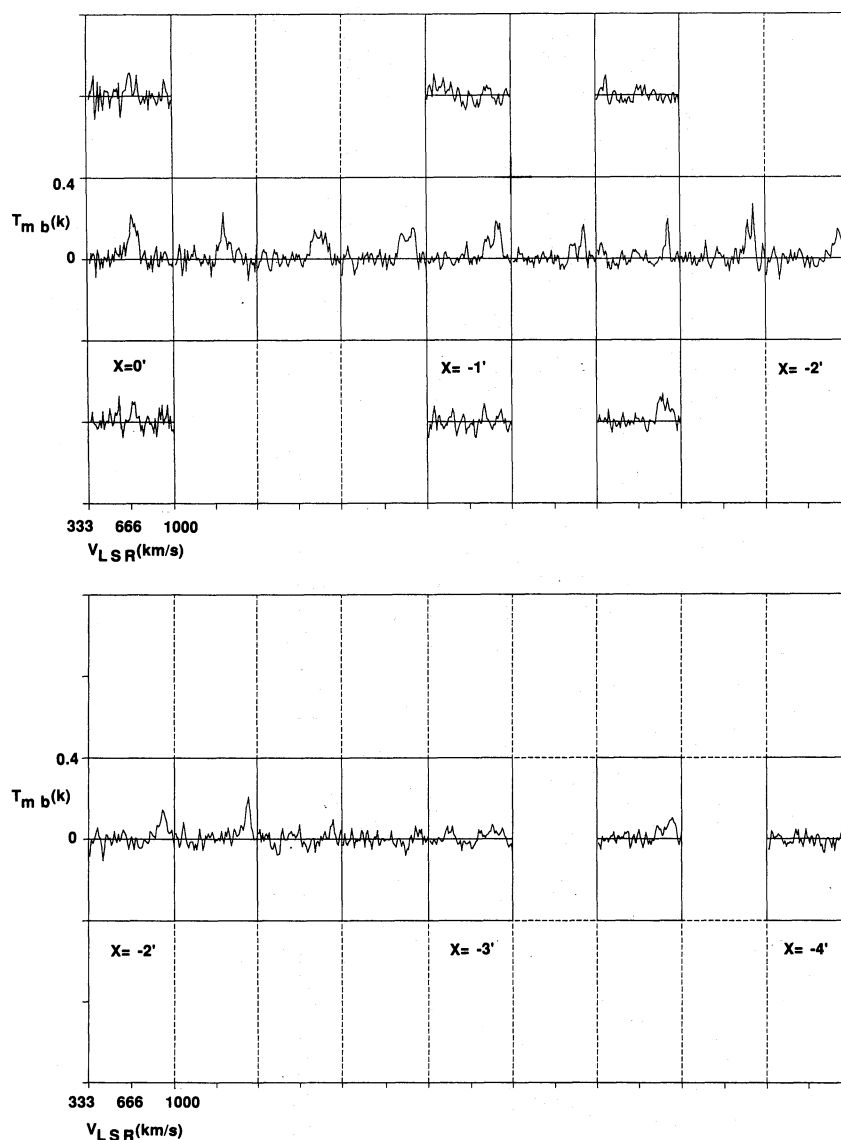


Fig. 1. (Continued)

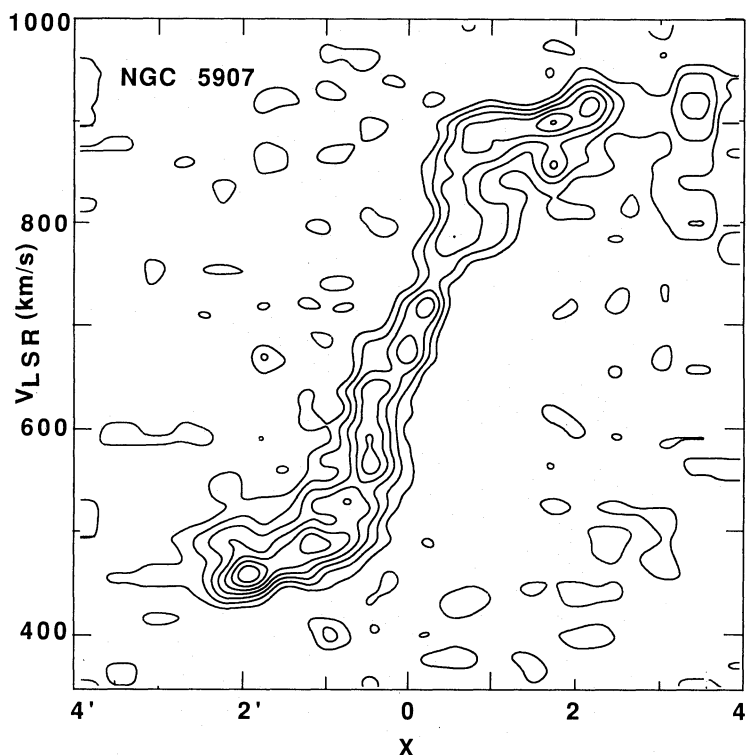


Fig. 2. Position-velocity ( $X-V$ ) diagram along the major axis of NGC 5907. The resolution is  $20'' \times 20 \text{ km s}^{-1}$ , and the rms noise of the map is about 13 mK in  $T_{\text{mb}}$ . Contours are drawn at every 20 mK in  $T_{\text{mb}}$  starting at 20 mK, and the peak intensity in the map is 245 mK  $T_{\text{mb}}$ .

smoothed to a resolution of  $20'' \times 20 \text{ km s}^{-1}$ . This yielded an rms noise of about 13 mK in  $T_{\text{mb}}$  on the PV map; the contours are drawn at every 20 mK  $T_{\text{mb}}$ . A rigid rotation feature is observed at  $|X| < 1'$  (3.4 kpc), which can be attributed to a molecular gas ring of radius 3 to 4 kpc. Beyond  $X \sim \pm 1'$ , the rotation velocity is almost constant, indicating flat rotation. By simply tracing the intensity maxima on the PV diagram, we found that flat rotation occurs at  $V_{\text{LSR}} = 460 \text{ km s}^{-1}$  and  $910 \text{ km s}^{-1}$ , which yields a rotation velocity of  $225 (\pm 10) \text{ km s}^{-1}$ .

Not like other "normal" edge-on Sb and Sc galaxies, such as the Milky Way (Dame et al. 1990), NGC 891, and NGC 4565 (Papers III and IV), no significant emission associated with nuclear rotating ring has been detected in the PV diagram. Such a depression of CO emission near to the center is exceptional for an Sc galaxy.

### 3.2. Intensity Distribution and Molecular Mass

The distribution of the integrated intensity,  $I_{\text{CO}} = \int T_{\text{mb}} dV$ , was obtained by integrating the PV diagram in  $V_{\text{LSR}}$ , and is shown in figure 3 as a function of  $X$ . This figure indicates a general concentration of CO gas on a ring at radius 1–2' (3–5 kpc). The distribution of radio continuum emission at 20 cm along the major axis is

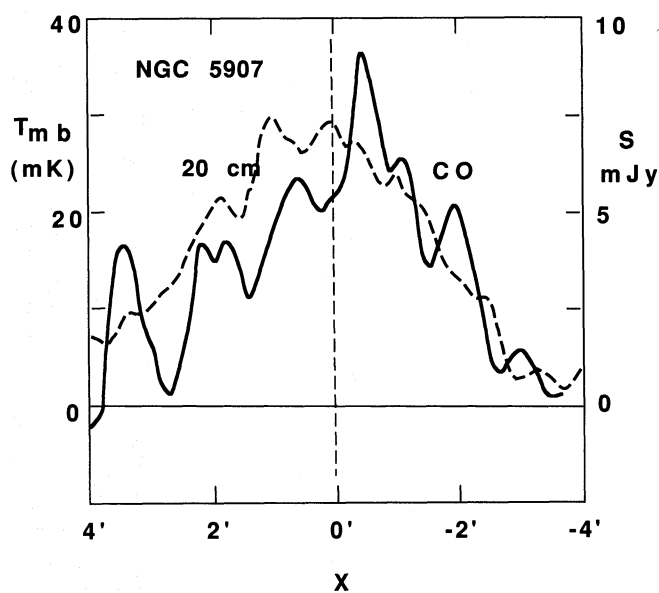


Fig. 3.  $I_{\text{CO}}$  distribution along the major axis  $X$  (full line). The resolution in the  $X$  direction is  $20''$ . Intensity of 20-cm continuum emission (resolution  $28''$ ; Hummel et al. 1984) is superposed by a dashed line.

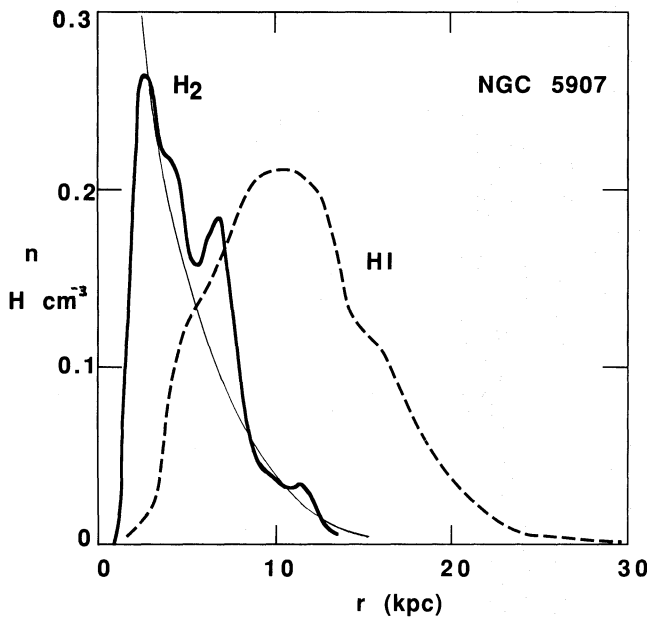


Fig. 4. Beam-diluted spatial densities of molecular (thick line) and neutral hydrogen (dashed line) gases (in  $\text{H cm}^{-3}$ ). The thin line shows an exponential-law disk with a scale radius 3.5 kpc fitted to the molecular gas distribution.

reproduced from Hummel et al. (1984), and is indicated by the dashed line in figure 3. We find a global correlation between the CO and continuum. It is also interesting to note that the galaxy has no radio continuum core, which is significantly different from other edge-on galaxies like NGC 891 and NGC 4565 (Hummel et al. 1984).

By integrating the CO emission in figure 2, we estimated the total CO luminosity of the observed region at  $-4' < X < 4'$  and  $-7.''5 < Y < 7.''5$  (within  $\pm 13.5$  kpc radius and  $\pm 422$  pc thickness) to be  $L_{\text{CO}} = 2.41(\pm 0.09) \times 10^8 \text{ K km s}^{-1} \text{ pc}^2$ . If we assume an  $\text{H}_2$  column density-to-CO intensity conversion factor of  $C = 3.6 \times 10^{20} \text{ H}_2 \text{ cm}^{-2} / \text{K km s}^{-1}$  (Sanders et al. 1984), the luminosity can be related to the  $\text{H}_2$  mass as  $M_{\text{H}_2} = 5.7 L_{\text{CO}}$ . Then, the total mass of  $\text{H}_2$  gas within the disk is estimated to be  $M_{\text{H}_2} = 1.37(\pm 0.05) \times 10^9 M_{\odot}$ .

### 3.3. Radial Distribution and the Molecular Front

By applying the simple decoding method of the integrated CO intensity around the terminal velocity, as proposed in Papers III and IV, we derived the radial distributions of the gaseous surface density as well as the beam-diluted spatial density. Here, we took a rotation velocity of  $V_{\text{rot}} = 225 \text{ km s}^{-1}$ . The minimum and maximum velocities of the integration were taken to be

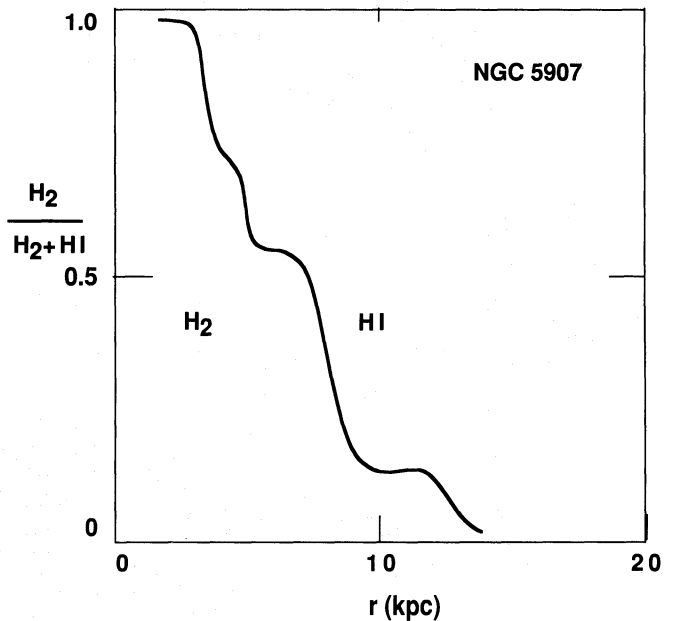


Fig. 5. Mass ratio of  $\text{H}_2$  to the total ( $\text{HI} + \text{H}_2$ ) gas density as a function of the galactocentric distance.

$V_{\text{min}} = 190$  and  $V_{\text{max}} = 250$ , respectively. Figure 4 shows the thus-obtained distribution of the spatial density of the molecular gas as a function of the radius. Here, the “beam-diluted” spatial density is defined by the surface density divided by the linear beam size of the observations. The density distribution can be approximately represented by the superposition of an exponential-law disk with a scale radius of 3.5 kpc, as indicated by the dotted line in figure 4, and a ring of radius 7 kpc. A striking feature in this figure is the sharp depression of the molecular gas near to the center, which will be discussed in subsection 3.5.

We apply this decoding method to the HI position-velocity diagram as presented by Casertano (1983). In figure 4 we plot the thus-obtained HI density by a dashed line. The HI distribution has a broad ring of 10 kpc radius associated with an outskirts reaching as far as 22 kpc radius. On the other hand, HI is deficient in the central several kpc. As shown in figure 4, the HI and  $\text{H}_2$  gases seem to be present at different radii, clearly avoiding each other. Figure 5 plots the mass ratio of the  $\text{H}_2$  gas density to the total ( $\text{HI} + \text{H}_2$ ) gas density. The HI gas is dominant in the outer region beyond 5 kpc, while  $\text{H}_2$  is dominant in the inner region. Particularly in the inner 4 kpc region, the gas is almost totally molecular. The “exchange” from HI to  $\text{H}_2$  appears to occur in coincidence with the molecular gas ring. As discussed in Paper IV in detail, we may be able to interpret this diagram in terms of the existence of a “molecular front”, at which the HI gas is

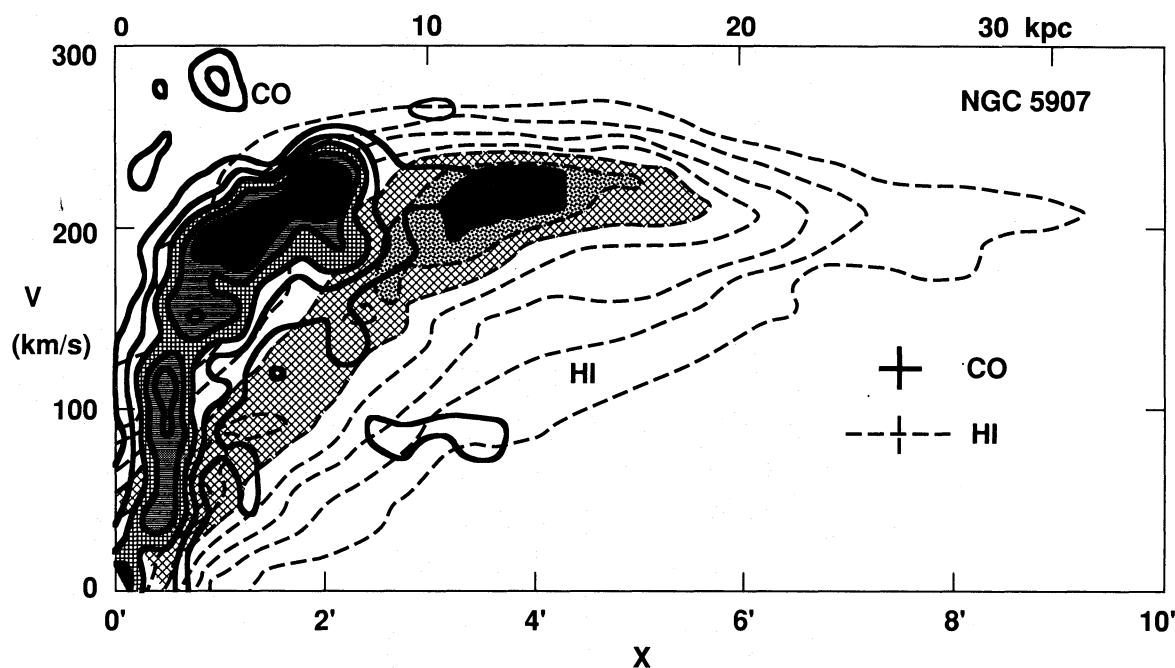


Fig. 6. Comparison of the CO and HI distributions on a PV diagram. A displacement of both species is shown here most clearly.

converted to  $H_2$ , or vice versa. This front may be the place where the galactic-scale phase change between HI and  $H_2$  is taking place, and would be deeply coupled with the evolution of interstellar gas.

#### 3.4. CO vs HI

In figure 6 we superpose the CO PV diagram on the HI PV diagram for the south-eastern side of NGC 5907, where the HI data are taken from Casertano (1983). This diagram demonstrates the clear displacement of molecular and atomic hydrogen gases. The HI gas comprises a large-diameter ring of 12 kpc radius, while molecular gas is distributed in the inner region at the 2 to 10 kpc radius region. It is remarkable that both gases are distributed while clearly avoiding each other: the inner region is dominated by molecular gas, and the outer region by HI. In both cases, the rigid-rotation features are due to the molecular and HI gas rings at these radii. As already discussed in subsection 3.3, it is also clearly observed in this figure that both emissions have a central depression.

Figure 6 indicates that the CO rotation velocity already attains a maximum at  $r \sim 3-6$  kpc, and is followed by a flat rotation of the outer HI gas. The fact that the HI and CO rotations attain the same maximum velocity at  $r \sim 5-10$  kpc can be used to argue for the coincidence of the total line profiles of both emissions: Fig-

ure 7 shows the "total line profile" in CO for NGC 5907, which was obtained by integrating the PV diagram in the X direction, and an HI profile as reproduced from Staveley-Smith and Davies (1988) is superposed. The figure indicates that the shapes and line widths of the HI and CO line profiles coincide remarkably well, although the spatial distributions of both species are significantly displaced. The total CO velocity width at the 20% level of the peak intensity was measured to be  $490 \pm 10$  km s $^{-1}$ , and is about equal to that obtained for the HI emission of 480 km s $^{-1}$ . This is consistent with the argument that the total CO line profiles of galaxies can be used as an alternative to the HI Tully-Fisher (1977) relation, as has been discussed in the case of NGC 891 (Sofue, Nakai 1992) and for other galaxies (Sofue 1992; Schöniger, Sofue 1993).

#### 3.5. Central Molecular Depression: Merger in the Bulge?

The conspicuous feature observed in figure 4 is the lack in CO emission near to the center, indicating a deficiency of the interstellar gas near the nucleus. Such a clear depression of the central molecular gas is exceptional for a Sc galaxy, and appears to be the first case among many late type spiral galaxies so far observed in CC as well as in HI. In fact, most Sc galaxies show a substantial concentration of CO emission toward the nucleus, comprising

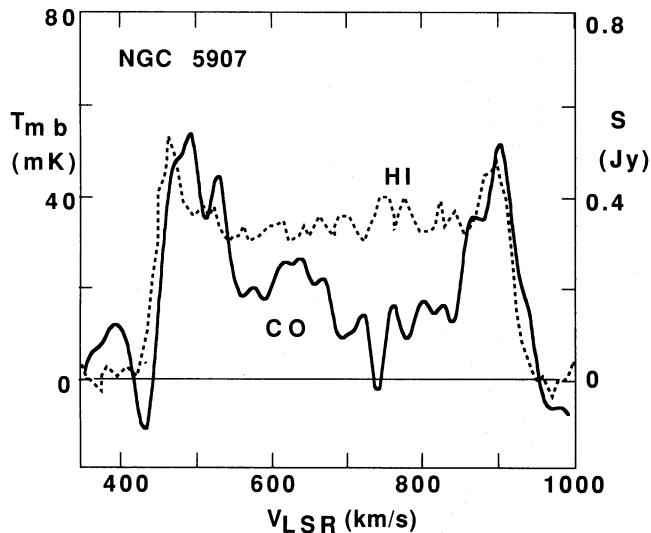


Fig. 7. Total line profile of the  $^{12}\text{CO}(J=1-0)$  emission along the major axis. The velocity resolution in this diagram is  $10 \text{ km s}^{-1}$ . An HI total line profile is indicated by the dashed line (Staveley-Smith, Davies 1988).

an exponential-law disk (Young, Scoville 1991; Sofue et al 1988).

M31 is the only example that was found to exhibit a similar central deficiency in interstellar gas (Brinks, Shane 1984; Koper et al. 1991; Sofue, Yoshida 1993): This giant Sb galaxy is characterized by its 10-kpc ring of interstellar gas and the "early-type" central bulge, which is anomalously deficient of interstellar gas. It has been suggested that the central gas depression in M31 would have been caused by a merger of another galaxy, by which the nuclear disk as well as the inner gas disk were destroyed through an angular momentum transfer as well as an accretion of gas from the merger galaxy (Sofue 1994). The merger in M31 has indeed been suggested to be the case due to the discovery of double nuclei with the Hubble Space Telescope (Lauer et al. 1993). Therefore, based on the similarity to M31,

we suggest that the nuclear gas disk of NGC 5907 was destroyed by a merger with another galaxy, probably a companion. In fact, the outer disk of NGC 5907 is significantly warped (Sancisi 1977), which could be evidence for a tidal disturbance which had occurred prior to the merger during a close encounter of both galaxies.

The author thanks Dr N. Nakai and the staff at NRO for their help during the observations.

## References

- Barnaby D., Thronson H.A.Jr 1992, AJ 103, 41  
 Bosma A.H. 1981, AJ 86, 1825  
 Braine J., Combes F., Casoli F., Durpaz C., Gerin M., Klein U., Wielebinski R., Brouillet N. 1993, A&AS 97, 887  
 Brinks E., Shane W.W. 1984, A&AS 55, 179  
 Casertano S. 1983, MNRAS 203, 735  
 Dame T.M., Ungerechts H., Cohen R.S., de Geus E.J., Grenier I.A., May J., Murphy D.C., Nyman L.-A et al. 1987, ApJ 322, 706  
 Hummel E., Sancisi R., Ekers R.D. 1984, A&A 133, 1  
 Koper E., Dame T.M., Israel F.P., Thaddeus P. 1991, ApJL 383, L11  
 Lauer, T., Faber, S. et al. 1993, AJ 106, 1436  
 Rots A. 1980, A&AS 41, 189  
 Sancisi R. 1977, in Topics in Interstellar Matter, ed H. van Woerden (Reidel, Dordrecht) p255  
 Sasaki T. 1987, PASJ 39, 849  
 Sanders D.B., Solomon P.M., Scoville N.Z. 1984, ApJ 276, 182  
 Schöniger F., Sofue Y. 1994, A&A in press  
 Sofue Y. 1991, PASJ 43, 671  
 Sofue Y. 1992, PASJ 44, L231  
 Sofue Y. 1994, ApJ 423, 207  
 Sofue Y., Doi M., Ishizuki S., Nakai N., Handa T. 1988, PASJ 40, 511  
 Sofue Y., Handa T., Nakai N. 1989, PASJ 41, 937 (Paper II)  
 Sofue Y., Nakai N. 1993, PASJ 45, 139 (Paper III)  
 Sofue Y., Nakai N. 1994, PASJ 46, 147 (Paper IV)  
 Sofue Y., Nakai N., Handa T. 1987, PASJ 39, 47 (Paper I)  
 Sofue Y., Yoshida S. 1994, ApJL 417, L63  
 Staveley-Smith L., Davies R.D. 1988, MNRAS 231, 833  
 Tully R.B., Fisher J.R. 1977, A&A 54, 661  
 Young J., Scoville N.Z. 1991, ARA&A 29, 581

